International Journal of Advanced Research in Biological Sciences
ISSN: 2348-8069
www.ijarbs.com
(A Peer Reviewed, Referred, Indexed and Open Access Journal)
DOI: 10.22192/ijarbs Coden: IJARQG (USA) Volume 13, Issue 1-2026

Research Article

DOI: http://dx.doi.org/10.22192/ijarbs.2026.13.01.001

Antimicrobial effects of *Irvingia gabonensis* peel extract - Synthesized silver nanoparticles

Anene I.C[1]., Emejulu A.A[1]., Anene C.C[2]. , Oghonim P.AN[3], Ovowa O.F[4]., Victor-Aduloju A.T[5]., Abana, C.C.[2], Egwuatu C.I[6]. , Umeoduagu N.D.[7], Okonkwo N.N.[2], Ebo P.U. [7]Igwilo C.Q.[2] and Agu, K.C.

[1]Department of Biochemistry, School of Biological Sciences,
Federal University of Technology, Owerri
[2]Department of Applied Microbiology, Nnamdi Azikiwe University, PMB 5025, Awka
[3]Microbiology Department, Biological Sciences, University of Delta,
Agbor P.M.B 2090, Agbor, Delta State, Nigeria
[4]Department of Science Laboratory Technology, Southern Delta University,
PMB 05, Ozoro, Delta State, Nigeria
[5]Department of Food Science and Technology, Nnamdi Azikiwe University, PMB 5025,
Awka[6]Department of Pure and Industrial Chemistry, Nnamdi Azikiwe University,
PMB 5025, Awka
[7]Department of Microbiology, Faculty of Natural and Applied Sciences, Tansian University,
Umunya,
Correspondence: *ifeanyichinaza759@gmail.com*

Abstract

The present study was aimed at the synthesis of silver nanoparticles using *Irvingia gabonensis* peel extracts and investigation of the antimicrobial effects of these nanoparticles against *Pseudomonas aeruginosa* and *Staphylococcus aureus* microorganisms. The fruits were harvested, washed, peeled and dried for 12 weeks. Aqueous extracts of the fruit peel samples were thereafter obtained and the synthesis of the silver nanoparticles was carried out by mixing 30 ml of aqueous extract with 70 ml of 4mM and 8mM concentrations respectively, of the silver trioxonitrate salt. The synthesized silver nanoparticles were characterized using UV-Visible spectroscopy. The *Irvingia gabonensis* peel extracts-synthesized silver nanoparticles exhibited potent antibacterial activity against *Pseudomonas aeruginosa* and *Staphylococcus aureus* microorganisms Results from the UV-Visible spectroscopy characterization confirmed the

synthesis of silver nanoparticles with spectral peaks obtained (between 200 and 429 nm) within the range expected for silver nanoparticles (between 380-480 nm). The silver nanoparticles synthesized using 4mM silver trioxonitrate salt was found to exhibit potent antibacterial activity with IC_{50} values of 38.05 µg/ml and 75.42µg/mlfor inhibition of total dehdrogenase activity of *Staphylococcus aureus* and*Pseudomonas aeruginosa* microorganisms respectively. IC_{50} values for the Inhibition of total dehydrogenase activity by the silver nanoparticles synthesized using 8mM silver trioxonitrate salt was not determinable. The results of this study thus have shown that silver nanoparticles can be synthesized using *Irvingiagabonensis*peel extracts and the silver nanoparticles possess significant antibacterial properties against *Staphylococcus aureus* and *Pseudomonas aeruginosa.*

Keywords: Antimicrobial, *Irvingia gabonensis,* Peel, Extract, Silver, Nanoparticles

Introduction

The expanding range of applications associated with nanoparticles has stimulated sustained scientific interest in nanotechnology, positioning it as one of the most rapidly advancing interdisciplinary research fields. Progress in nanoscience has significantly reshaped modern approaches to disease diagnosis, prevention, and therapy, while also enabling innovative solutions in environmental remediation and industrial processes. Consequently, engineered nanoparticles and nanomaterials within the size range of 1–100 nm have become a focal point of contemporary research due to their extensive utility across medicine, engineering, and applied sciences (Lin et al., 2014). Nanoparticles are broadly characterized as materials possessing at least one dimension within the nanoscale domain, a feature that imparts properties distinctly different from those of their bulk counterparts. Their remarkably high surface-area-to-volume ratio is responsible for enhanced chemical activity and distinctive optical, mechanical, magnetic, and electronic behaviors (Vithiya & Sen, 2011). Furthermore, the dimensional similarity between nanoparticles and biological macromolecules such as proteins and nucleic acids facilitates close biological interactions, thereby enhancing their functional relevance in biomedical applications (Ingale & Chaudhari, 2013).

The unique performance of nanomaterials compared with conventional bulk materials is primarily governed by surface-related phenomena and quantum confinement effects. These factors collectively influence physicochemical properties, including reactivity, tensile strength, optical absorption, electrical conductivity, and magnetic response (Buzea et al., 2007). Such attributes underpin the growing interest in nanomaterials for biomedical use, particularly in antimicrobial applications, where nanoscale interactions can compromise microbial cell integrity and interfere with vital metabolic functions. Within this framework, nanotechnology-driven antimicrobial approaches are increasingly being explored as effective alternatives to traditional antibiotics, especially in response to the global rise in antimicrobial resistance (Morones et al., 2005; Agu et al., 2013; Awah et al., 2017).

In parallel, the synthesis of nanoparticles using environmentally benign methods has gained considerable attention. Green synthesis routes are widely favored because they require fewer hazardous chemicals, are cost-efficient, and align with principles of environmental sustainability. The use of biological macromolecules that serve simultaneously as reducing, stabilizing, and capping agents further enhances the appeal of these approaches (Lateef et al., 2016). Conversely, physical fabrication techniques such as vapor deposition and molecular beam epitaxy demand sophisticated infrastructure and high energy input, while many chemical synthesis methods rely on toxic reagents that limit their suitability for biomedical applications (Garg, 2012). As a result, biologically mediated synthesis pathways have emerged as safer and more sustainable alternatives, particularly for antimicrobial and medical uses.

Extensive studies have demonstrated that biological systems can act as effective "natural reactors" for the formation of metal and metal oxide nanoparticles through biomimetic mechanisms. A wide array of biological resources including bacteria, fungi, yeasts, plant extracts, and agricultural residues has been successfully employed as eco-friendly substrates for nanoparticle production (Sharma et al., 2015). Among these options, plant-based synthesis has gained prominence due to its scalability, elimination of microbial culture maintenance, simplified downstream processing, and the multifunctional role of phytochemicals as both reducing and stabilizing agents. Consequently, phyto-mediated synthetic strategies have become increasingly popular. Different plant parts, such as leaves, fruits, bark, roots, peels, and callus tissues, are rich in secondary metabolites including flavonoids, phenolics, terpenoids, tannins, and plant enzymes that efficiently convert metal ions into stable nanoparticle forms (Das & Velusamy, 2013; Ubaoji et al., 2020).

The resurgence of interest in biologically synthesized nanoparticles is further driven by the escalating global burden of antimicrobial resistance. Excessive and inappropriate antibiotic use has accelerated the emergence of multidrug-resistant (MDR) bacterial strains, thereby severely constraining available treatment options (Awari et al., 2023; Umeoduagu et al., 2023). This problem is particularly severe for opportunistic pathogens such as *Staphylococcus aureus* and *Pseudomonas aeruginosa*, which are commonly implicated in both hospital- and community-acquired infections and exhibit resistance to multiple antibiotic classes (Archer, 2018; Linden et al., 2013). Accordingly, several studies have emphasized the urgent need for alternative antimicrobial strategies, including those based on plant-derived bioactive compounds, probiotic systems, and nanomaterial-based interventions (Agu et al., 2014; Ravindran et al., 2016; Obasi et al., 2024).

Irvingia gabonensis, commonly referred to as bush mango or wild mango, is a widely consumed non-timber forest product across Nigeria and other regions of West and Central Africa. The plant has attracted significant scientific interest due to its rich phytochemical profile and broad spectrum of medicinal applications (Ekundayo et al., 2013; Etta et al., 2014). Traditionally, various parts of the plant are used in the management of infections, wounds, gastrointestinal ailments, and metabolic disorders. Phytochemical investigations have revealed that *I. gabonensis* contains bioactive constituents such as flavonoids, tannins, saponins, steroids, and glycosides, which are associated with antioxidant, antimicrobial, antiviral, hypoglycemic, and anti-inflammatory activities (Ewere et al., 2017; Oben, 2010; Hossain et al., 2012).

Importantly, extracts derived from *I. gabonensis* have demonstrated inhibitory effects against several pathogenic microorganisms, including in vitro suppression of HIV, mediated through disruption of glycoprotein processing and host-cell attachment mechanisms (Raji et al., 2001). These findings, together with accumulating evidence supporting the antimicrobial efficacy of other plant-based products (Okigbo et al., 2015; Awah et al., 2016; Umeoduagu et al., 2023), justify further exploration of *I. gabonensis* as a sustainable bioresource for green nanoparticle synthesis with antimicrobial potential.

Given the increasing incidence of MDR bacterial infections—particularly those caused by *S. aureus* and *P. aeruginosa*—and the demonstrated bioactivity of plant-derived compounds, the development of environmentally friendly nanoparticle-based antimicrobial agents represents a promising and timely research direction. This rationale forms the foundation of the present investigation.

Accordingly, this study focuses on the green synthesis of silver nanoparticles using aqueous peel extracts of *Irvingia gabonensis* and the evaluation of their antibacterial efficacy against *Staphylococcus aureus* and *Pseudomonas aeruginosa*. To the best of available knowledge, this work constitutes the first reported attempt to synthesize silver nanoparticles using *I. gabonensis* peel extracts via an eco-friendly approach.

Materials and Methods

Collection and Authentication of Plant Material

Fresh fruits of *Irvingia gabonensis* were obtained from Ihiagwa Market, located in Owerri, Imo State, Nigeria. Botanical identification and authentication of the plant material were performed by Dr. F. N. Mbagwu, a taxonomist in the Department of Plant Science and Biotechnology, Imo State University, Owerri. A representative specimen was deposited in the university herbarium and assigned the voucher number IMSUH 0198 for future reference.

Processing of Plant Samples

The harvested fruits were thoroughly rinsed under running tap water to remove adhering debris. The outer peels were carefully separated using a sterile stainless-steel knife. The peels were air-dried at ambient laboratory temperature in a well-ventilated environment, shielded from direct sunlight, for a duration of twelve weeks. Following complete drying, the samples were pulverized into fine powder using a manual grinding apparatus and stored in clean, dry sample containers until required for extraction.

Preparation of Aqueous Extract

A measured quantity of 50 g of the powdered peel material was weighed using an electronic balance and transferred into a conical flask containing 500 mL of distilled water. The mixture was heated to boiling and maintained for one hour to facilitate extraction of bioactive constituents. The resulting decoction was allowed to cool to room temperature and subsequently passed through a mucilage sieve to remove coarse particles. Further clarification was achieved by filtration through Whatman No. 1 filter paper. The clarified filtrate was stored at 4°C pending further use.

Biosynthesis of Silver Nanoparticles

For nanoparticle synthesis, aqueous solutions of silver trioxonitrate were prepared at concentrations of 4 mM and 8 mM by dissolving 0.07 g and 0.14 g of the salt, respectively, in 100 mL of distilled water. Each solution was stirred continuously for 30 minutes using a magnetic stirrer to ensure complete dissolution. Subsequently, 30 mL of the prepared plant extract was added to 70 mL of each silver trioxonitrate solution. The reaction mixtures were left undisturbed at room temperature for 72 hours to allow complete reduction of silver ions and sedimentation of the formed nanoparticles. After incubation, the mixtures were oven-dried for approximately three hours to remove residual moisture. The dried silver nanoparticle residues were gently scraped from the reaction vessels and transferred into labeled Eppendorf tubes for storage.

UV–Visible Spectroscopic Characterization

Optical characterization of the synthesized silver nanoparticles was conducted using a UV–Visible spectrophotometer (Shimadzu UV-7000 series). Approximately 0.2 g of the nanoparticle sample obtained from each silver trioxonitrate concentration was dispersed in 2 mL of distilled water. The absorbance spectra of the suspensions were recorded across the UV–Visible range, and the resulting spectral data were documented for analysis.

Evaluation of Antibacterial Activity

The antibacterial efficacy of the synthesized nanoparticles and plant extract was assessed using the total dehydrogenase inhibition assay, following the procedure described by Alisi et al. (2008). The assay was based on the reduction of 2,3,5-triphenyltetrazolium chloride (TTC) to the red-coloredtriphenyl formazan (TPF), which served as an indicator of metabolic activity. Test reactions were set up in 2 mL volumes of nutrient broth–TTC medium containing graded

concentrations of silver nanoparticles (0–300 µg/mL) and *I. gabonensis* peel or leaf aqueous extracts (0–3000 µg/mL) in separate 10 mL screw-capped test tubes.

To achieve the desired concentrations, 0.5 mL of standard nutrient broth was combined with appropriate volumes of distilled water and either nanoparticle stock solution (500 µg/mL) or extract stock solution (5000 µg/mL). Each tube received 0.1 mL of 0.1% (w/v) TTC prepared in deionized distilled water, followed by the addition of 0.1 mL of a standardized bacterial suspension. Control setups containing inoculated media without nanoparticles or extracts were included. All tubes were properly labeled and incubated at room temperature (28 ± 2°C) for 24 hours. After incubation, the produced TPF was extracted with 4 mL of butanol, and absorbance was measured at 500 nm using a Vis 721D spectrophotometer.

Statistical Analysis

UV–Visible spectral profiles corresponding to nanoparticles synthesized using 4 mM and 8 mM silver trioxonitrate were obtained directly from the spectrophotometer. The extent of dehydrogenase inhibition induced by the nanoparticles and extracts was calculated relative to the untreated control. Percentage inhibition values were plotted against corresponding concentrations using Table 2D Curve software (Version 5.01). From the resulting dose–response curves, inhibitory concentration thresholds (IC_5, IC_{10}, IC_{20}, IC_{50}, IC_{80}, and IC_{100}) were determined.

Results

UV–Visible Spectral Analysis of Silver Nanoparticles

Presented below are the UV–Visible absorption spectra illustrating the characteristic plasmon resonance peaks of silver nanoparticles synthesized using 4 mM and 8 mM silver trioxonitrate solutions.

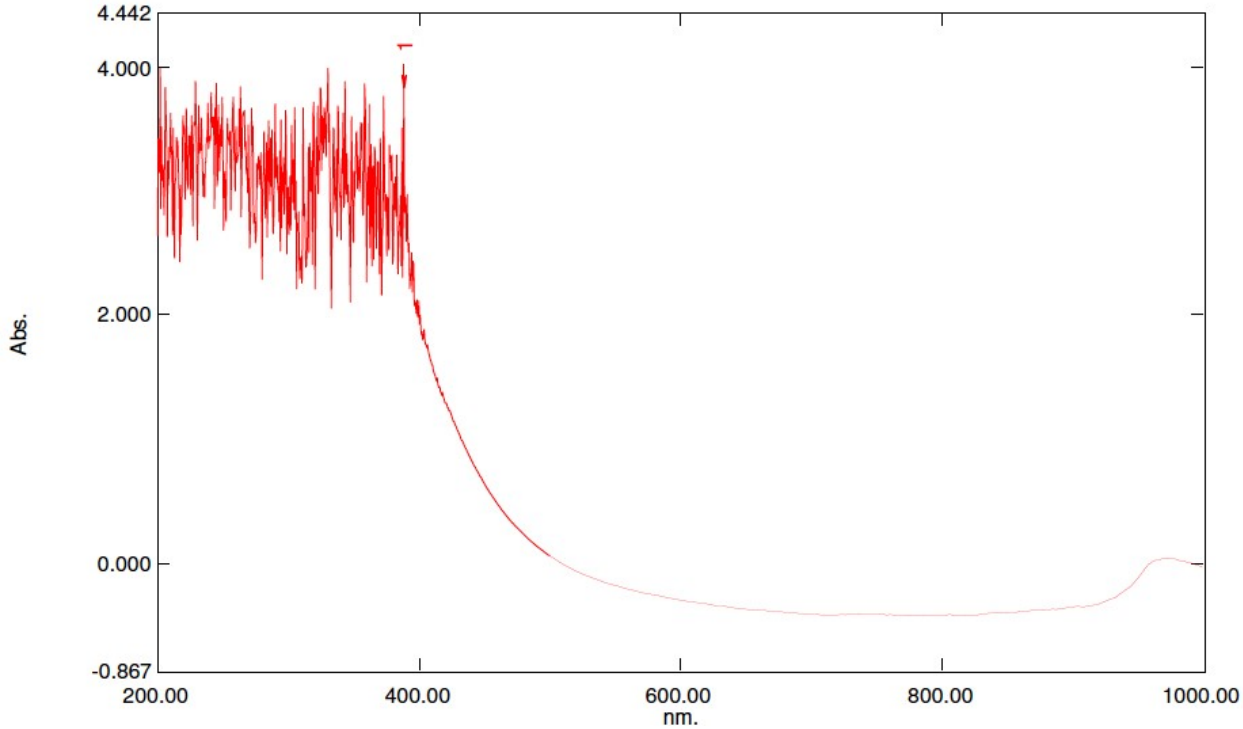

Fig. 1: Spectrum peak report of the UV-Visible characterization of the silver nanoparticles synthesized using 4mM silver trioxonitrate salt and peel aqueous extract of *I. gabonensis.*

As shown in fig. 1, the silver nanoparticles synthesized using 4mM silver trioxonitrate salt showed produced several spectral peaks between 200 and 400nm.

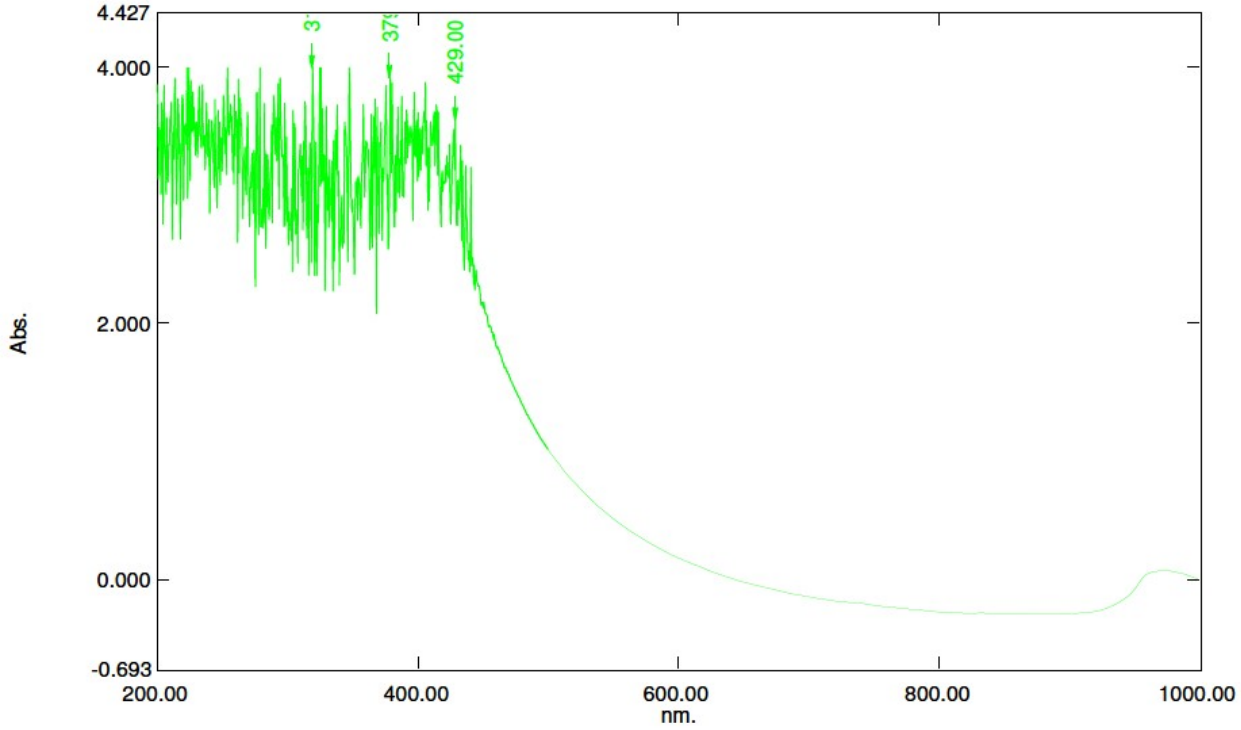

Fig. 2: Spectrum peak report of the UV-Visible characterization of the silver nanoparticles synthesized using 8mM silver trioxonitrate salt and peel aqueous extract of *I. gabonensis.*

Fig. 2 depicts the spectral peak report of the silver nanoparticles synthesized using 4mM silver trioxonitrate salt and peel aqueous extract of *I. gabonensis*. Several peaks were observed between 200 and 441nm.

1.2.2 Antimicrobial activity of the silver nanoparticles

The tables below shows the inhibitory concentrations of the *Irvingia gabonensis* crude peel extracts and silver nanopaticles against *Staphylococcus aureus* and *P. aeruginosa* microorganisms.

Table 1: Threshold inhibitory concentrations of the *Irvingia gabonensis* aqueous crude peel extracts and silver nanoparticles against *Staphylococcus aureus*

Samples	Inhibitory concentrations of extracts (µg/ml)				
	IC_{20}	IC_{40}	IC_{50}	IC_{60}	IC_{80}
Peel nanoparticle (4mM)	30.08	34.16	38.05	43.78	65.86
Peel nanoparticle (8mM)	90.70	ND	ND	ND	ND
Crude peel extract	51.63	246.12	454.59	799.89	2329.89
Ciprofloxacin (standard)	6.05	11.87	15.34	19.73	36.90

Key: ND = Not determinable

According to the table above, the silver nanoparticles synthesized using 4mM concentration of the silver salt had an IC_{50} value of 38.05 µg/ml whereas IC_{50} was not determinable for the silver nanoparticles synthesized using 8mM concentration of silver trioxonitrate salt. The table above also shows that the concentration of the aqueous peel extracts that exhibited 50% dehydrogenase inhibition activity (IC_{50}) in the *Staphylococcus aureus* was 454.59 µg/ml. The standard (Ciprofloxacin), however, had the lowest IC_{50} value of all the samples, with a value of 15.34 µg/ml.

Table 2: Threshold inhibitory concentrations of the *Irvingia gabonensis* aqueous crude peel extracts and silver nanoparticles against *Pseudomonas aeruginosa.*

Samples	Inhibitory concentrations of extracts (µg/ml)				
	IC_{20}	IC_{40}	IC_{50}	IC_{60}	IC_{80}
Peel nanoparticle (4mM)	15.69	43.97	75.42	160.56	ND
Peel nanoparticle (8mM)	102.64	ND	ND	ND	ND
Aqueous peel extract	503.86	1015.67	1462.63	2026.72	3488.54
Ciprofloxacin (standard)	6.86	14.62	20.17	27.72	56.54

Key: ND = Not determinable

An IC_{50} value of 75.42 µg/ml was got for the silver nanoparticles synthesized using 4mM concentration of the silver salt according to the table above. This value is lower than the IC_{50}valueof 1462.63 µg/ml which was obtained for the aqueous peel extract. The IC_{50} value for the silver nanoparticles synthesized using 8mM silver nitrate salt was not determinable. The standard, however, recorded the lowest IC_{50} value of 20.17 µg/ml.

These tables above were used in plotting graphs for the dehydrogenase inhibitory activities of the aqueous peel extract, silver nanoparticles synthesized using 4mM silver nitrate salt and 8mM silver nitrate salt resepectively, and standards against *S. aureus* and *P. aeruginosa* total dehydrogenase activity. These graphs are shown below.

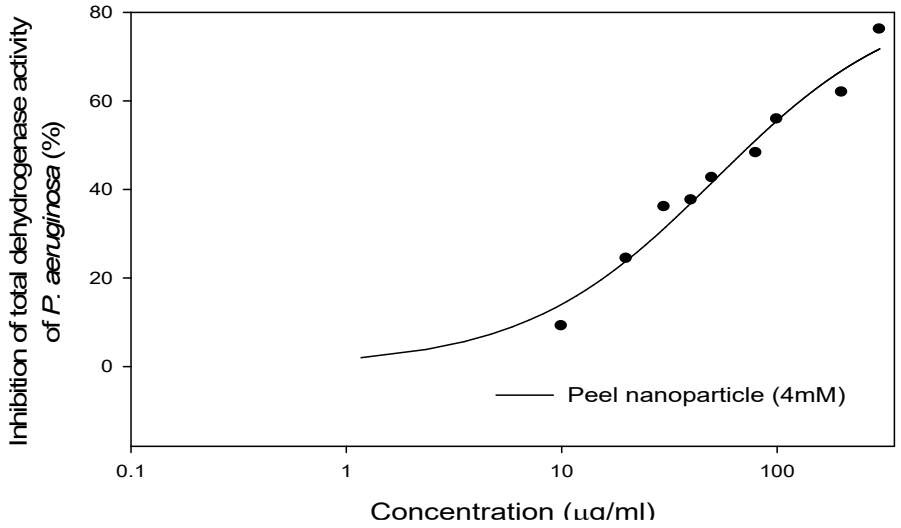

Fig.3: Graph of inhibition of total dehydrogenase activity of *P. aeruginosa* by the silver nanoparticles synthesized using 4mM silver nitrate salt and peel extract.

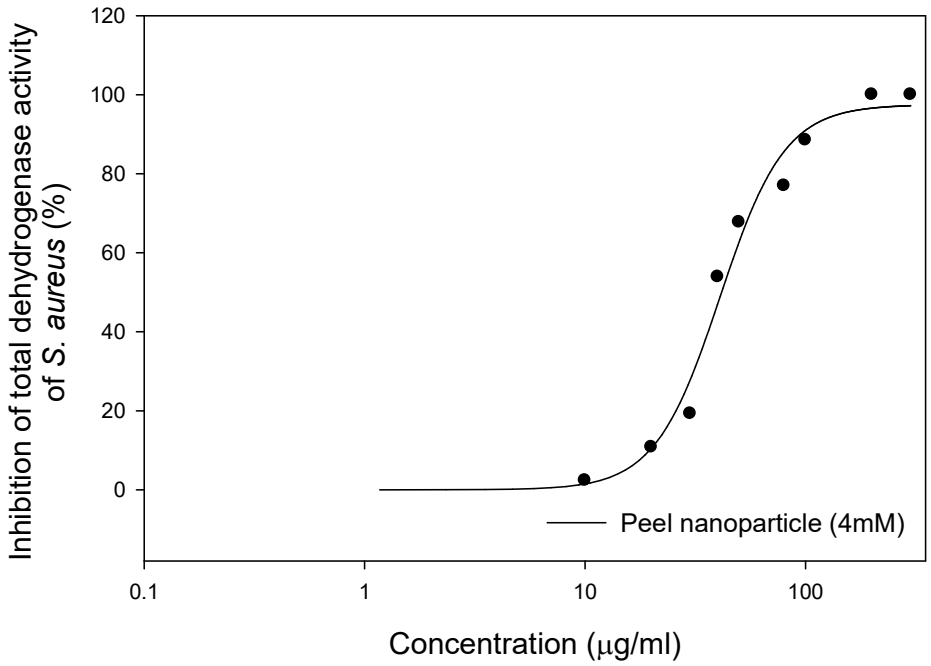

Fig.4: Graph of inhibition of total dehydrogenase activity of *S. aureus* by the silver nanoparticles synthesized using 4mM silver nitrate salt and peel extract.

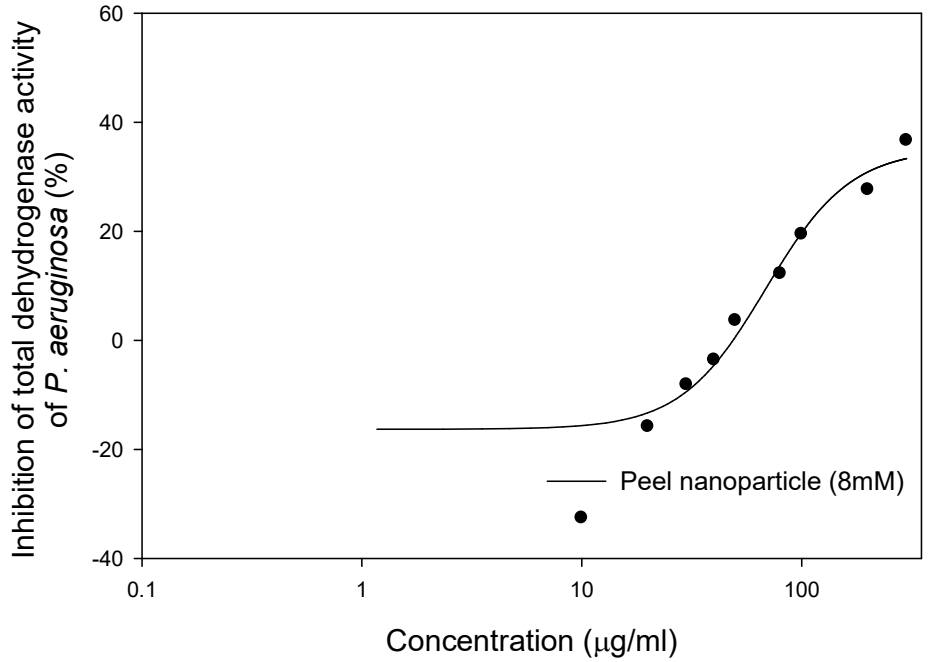

Fig.5: Graph of inhibition of total dehydrogenase activity of *P. aeruginosa* by the silver nanoparticles synthesized using 8mM silver nitrate salt and peel extract.

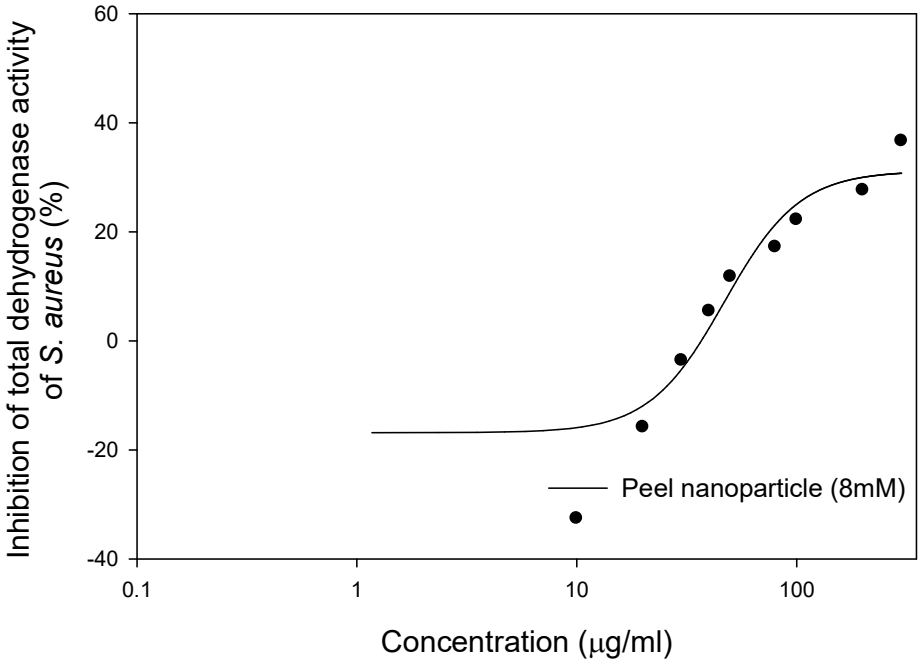

Fig.6: Graph of inhibition of total dehydrogenase activity of *S. aureus* by the silver nanoparticles synthesized using 8mM silver nitrate salt and peel extract

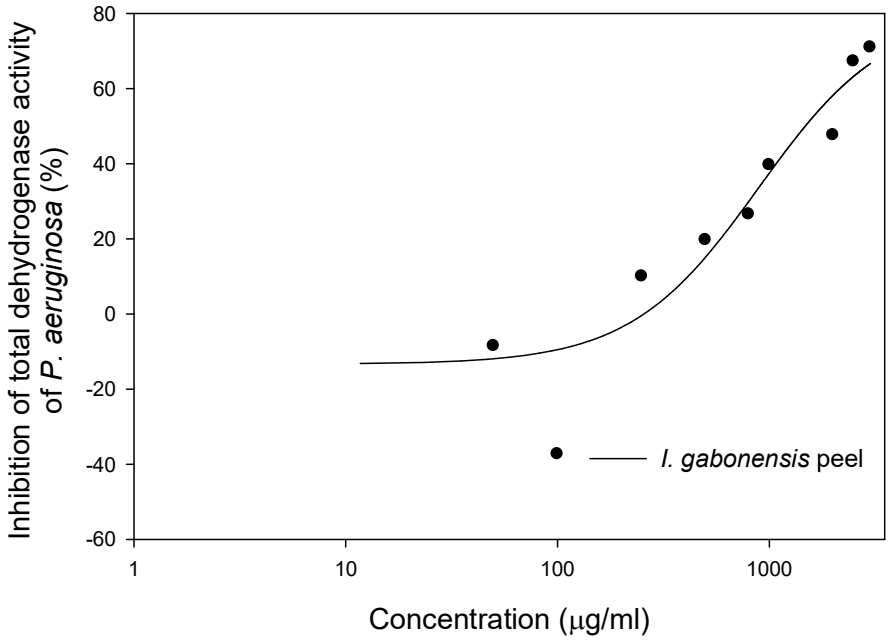

Fig.7: Graph of inhibition of total dehydrogenase activity of *P. aeruginosa* by the aqueous peel extract.

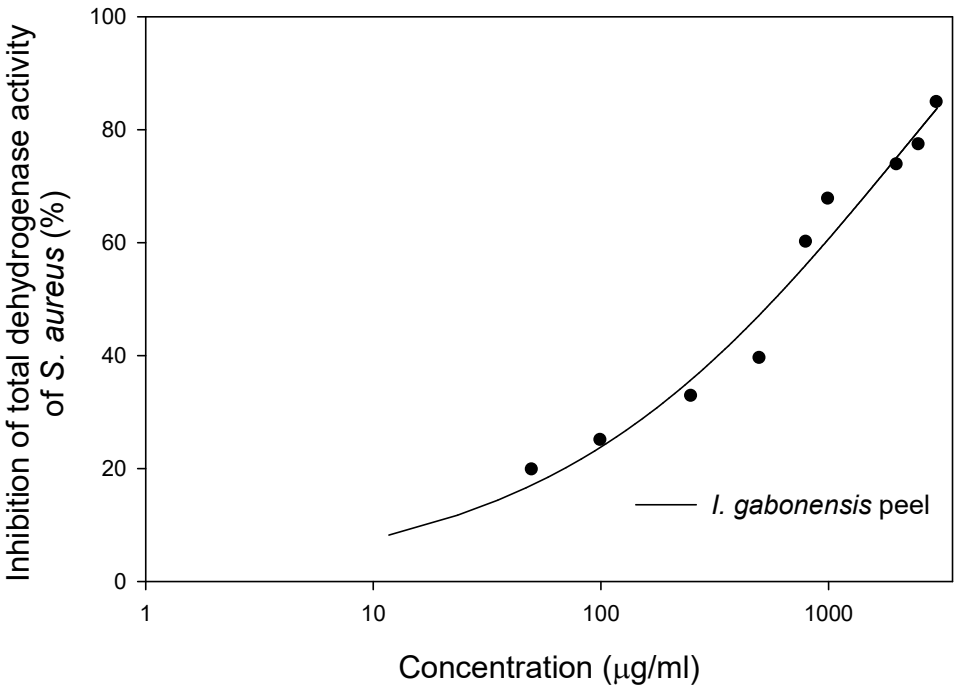

Fig.8: Graph of inhibition of total dehydrogenase activity of *S. aureus* by the aqueous peel extract.

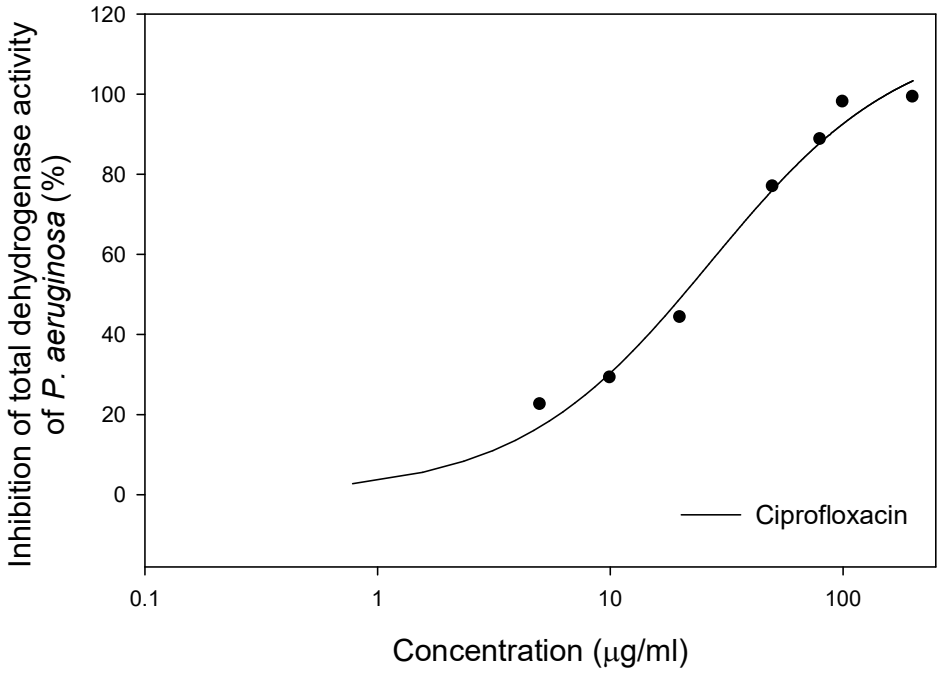

Fig.9: Graph of inhibition of total dehydrogenase activity of *P. aeruginosa* by the standard (ciprofloxacin).

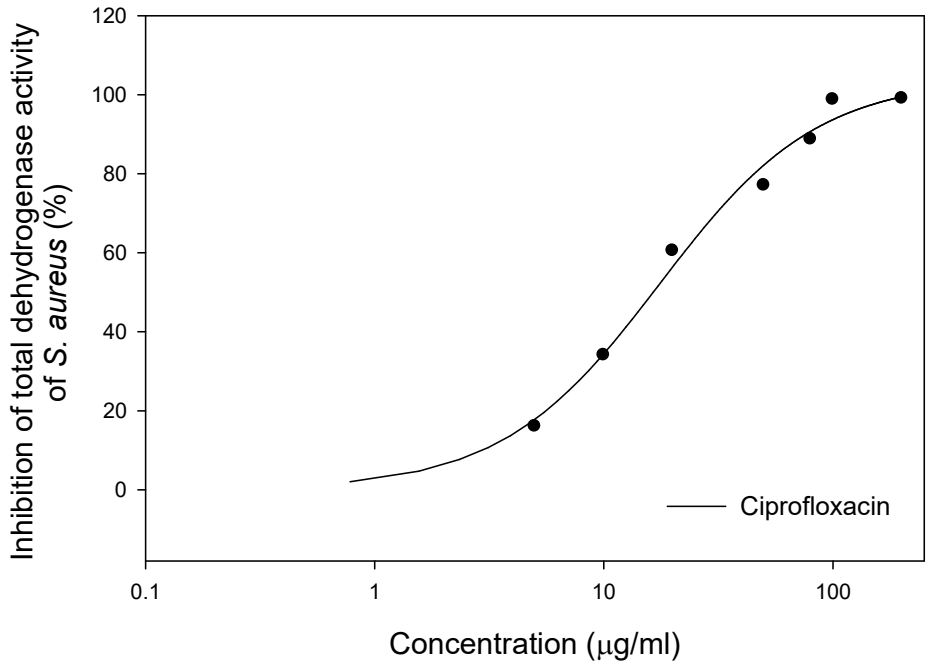

Fig.10: Graph of inhibition of total dehydrogenase activity of *S. aureus* by the standard (ciprofloxacin)

The graphical data illustrate the extent to which different test samples and the reference drug suppressed total dehydrogenase enzyme activity in *Pseudomonas aeruginosa* and *Staphylococcus aureus*. As presented in Figures 3 and 4, silver nanoparticles produced using a 4 mM silver nitrate precursor inhibited dehydrogenase activity in both bacterial species in a concentration-related fashion. Increasing nanoparticle concentrations resulted in progressively greater enzymatic inhibition in the tested organisms.

Figures 5 and 6 present the inhibitory effects of silver nanoparticles synthesized with an 8 mM silver salt concentration on the total dehydrogenase activity of *P. aeruginosa* and *S. aureus*, respectively. In both cases, inhibition increased with concentration up to approximately 120 µg/mL for *P. aeruginosa* and 100 µg/mL for *S. aureus*. At these concentrations, maximal inhibition of roughly 31% was observed, after which further increases in nanoparticle dosage did not produce additional inhibitory effects, indicating a plateau in activity.

Figures 7 and 8 demonstrate that the aqueous peel extract of *Irvingia gabonensis* also reduced total dehydrogenase activity in both bacterial species in a dose-responsive manner, with higher extract concentrations yielding greater inhibition. Similarly, Figures 9 and 10 show that the reference antibiotic, ciprofloxacin, exerted concentration-dependent suppression of dehydrogenase activity in *P. aeruginosa* and *S. aureus*, with increasing doses producing correspondingly higher levels of inhibition.

Discussion

In this investigation, silver nanoparticles were successfully biosynthesized using an aqueous extract derived from *Irvingia gabonensis* peels. The formation of nanoparticles was visually confirmed by a color transition in the reaction mixture from green to brown, a phenomenon commonly associated with the reduction of silver ions and nanoparticle formation. Over time, grayish precipitates accumulated at the bottom of the reaction vessel, while the supernatant retained its brown coloration. This pattern was observed regardless of whether 4 mM or 8 mM silver trioxonitrate was employed during synthesis.

Comparable observations have been reported by other researchers, who described similar precipitate formation and color changes during biologically mediated silver nanoparticle synthesis. Variations in observed coloration, ranging from yellowish-brown to dark greenish hues, have been attributed to differences in the nature and composition of biomolecules responsible for nanoparticle reduction and stabilization.

The conversion of silver ions (Ag^+) to elemental silver (Ag^0) nanoparticles is facilitated by phytochemicals present in the plant extract, which act as reducing and capping agents. *Irvingia gabonensis* peels are known to contain a diverse array of bioactive compounds, including flavonoids, tannins, saponins, alkaloids, terpenoids, steroids, volatile oils, and cardiac glycosides. These constituents are likely involved in electron donation and stabilization processes that drive nanoparticle formation. Previous studies have similarly identified polyphenols, sugars, proteins, enzymes, alkaloids, and other plant-derived metabolites as key contributors to the bioreduction of silver ions during green synthesis protocols.

Ultraviolet–visible (UV–Vis) spectroscopy remains a fundamental analytical technique for confirming nanoparticle synthesis and assessing their optical characteristics. In metallic nanoparticles such as silver, closely spaced conduction and valence bands allow free electrons to collectively oscillate in response to incident light, producing a characteristic surface plasmon resonance (SPR) absorption band.

In the present study, UV–Vis spectral analysis revealed distinct absorption peaks for silver nanoparticles synthesized with 4 mM silver trioxonitrate within the 200–400 nm wavelength range. Nanoparticles prepared using 8 mM silver salt exhibited similar absorption features, with peaks extending up to approximately 441 nm. These findings are consistent with previous reports indicating that silver nanoparticles typically display SPR bands between 380 and 480 nm.

The appearance of additional peaks outside this conventional SPR range may reflect particle aggregation, the presence of unreacted phytochemicals, or other particulate impurities within the reaction mixture. Increased silver salt concentrations have been associated with enhanced nanoparticle agglomeration due to elevated particle density, which promotes coalescence and the formation of larger particles. Such aggregation can lead to sedimentation and altered optical behavior, thereby contributing to spectral deviations beyond the expected SPR region.

Silver nanoparticles synthesized from *I. gabonensis* peels demonstrated pronounced antibacterial efficacy against *Staphylococcus aureus*, as assessed using the total dehydrogenase activity assay. Dehydrogenase enzymes play a central role in microbial metabolism and are rapidly degraded following cell death, making their activity a reliable indicator of bacterial viability.

The concentration of silver nanoparticles synthesized with 4 mM silver trioxonitrate required to inhibit 50% of dehydrogenase activity (IC_{50}) in *S. aureus* was determined to be 38.05 µg/mL. In contrast, an IC_{50} value could not be established for nanoparticles synthesized using 8 mM silver salt, likely due to nanoparticle aggregation that reduced bioavailability and enzymatic interaction. This aggregation phenomenon was also reflected in the complex UV–Vis spectral profiles observed for these samples.

Comparatively, the antibacterial reference drug ciprofloxacin exhibited a lower IC_{50} value (15.34 µg/mL), indicating greater potency, while the aqueous peel extract showed substantially weaker activity (IC_{50} = 454.59 µg/mL). These findings underscore the enhanced antibacterial performance of silver nanoparticles relative to the crude plant extract, although ciprofloxacin remained the most effective agent tested. Previous studies have likewise documented the inhibitory effects of silver nanoparticles on *S. aureus* growth and metabolism.

With respect to *Pseudomonas aeruginosa*, silver nanoparticles synthesized using 4 mM silver trioxonitrate displayed the strongest inhibitory effect among all test samples, aside from the standard antibiotic. An IC_{50} value of 75.42 µg/mL was recorded, demonstrating markedly higher potency than the aqueous peel extract, which exhibited an IC_{50} value exceeding 1400 µg/mL. These results further support the application of biosynthesized silver nanoparticles as effective antibacterial agents against *P. aeruginosa*, in agreement with earlier reports.

The antibacterial action of silver nanoparticles has been attributed to multiple mechanisms, including disruption of bacterial membrane integrity, interference with enzymatic systems, and inhibition of cellular respiration. Silver ions can induce potassium ion efflux and compromise membrane-associated enzymes and genetic material. Additionally, silver nanoparticles may generate reactive oxygen species that impair key respiratory enzymes, including lactate dehydrogenase, ultimately suppressing bacterial growth and replication. Penetration of the bacterial cell envelope by nanoparticles further contributes to membrane permeability loss and leakage of intracellular contents, culminating in metabolic collapse.

Conclusion

This study demonstrates that silver nanoparticles can be efficiently synthesized through a green approach employing *Irvingiagabonensis* peel extracts. The resulting nanoparticles exhibit strong antibacterial activity against *Staphylococcus aureus* and *Pseudomonas aeruginosa*, with significantly greater efficacy than the corresponding aqueous plant extract. These findings highlight the potential of plant-mediated silver nanoparticles as promising antibacterial agents.

References

Agu, K. C., Awah, N. S., Nnadozie, A. C., Okeke, B. C., Orji, M. U., Iloanusi, C. A., Anaukwu, C. G., Eneite, H. C., Ifediegwu, M. C., Umeoduagu, N. D., &Udoh, E. E. (2016). Isolation, identification and pathogenicity of fungi associated with cocoyam (*Colocasiaesculenta*) spoilage. *Food Science and Technology*, 4(5), 103–106. https://doi.org/10.13189/fst.2016.040503

Agu, K. C., Awah, N. S., Sampson, P. G., Ikele, M. O., Mbachu, A. E., Ojiagu, K. D., Okeke, C. B., Okoro, N. C. N., & Okafor, O. I. (2014). Identification and pathogenicity of rot-causing fungal pathogens associated with *Xanthosomas agittifolium* spoilage in southeastern Nigeria. *International Journal of Agriculture Innovations and Research*, 2(6), 1155–1159.

Agu, K. C., Igweoha, C. A., &Umeh, C. N. (2013). Antimicrobial activity of the ethanolic and petroleum ether extracts of tangerine seeds on selected bacteria. *International Journal of Agriculture and Bioscience*, 2(1), 22–24.

Akiyama, H., Fujii, K., Yamasaki, O., Oono, T., &Iwatsuki, K. (2001). Antibacterial action of several tannins against *Staphylococcus aureus*. *Journal of Antimicrobial Chemotherapy*, 48, 487–491.

Alisi, C. S., Nwanyanwu, C. E., Akujobi, C. O., &Ibegbulem, C. O. (2008). Inhibition of dehydrogenase activity in pathogenic bacterial isolates by aqueous extracts of *Musa paradisiaca* (var. sapientum). *African Journal of Biotechnology*, 7(12), 1821–1825.

Anazodo, C. A., Abana, C. C., Agu, K. C., Victor-Aduloju, A. T., Okoli, F. A., Ifediegwu, M. C., Awari, V. G., & Chidozie, C. P. (2024). *In vitro* antifungal efficacy of *Allium cepa* and *Allium sativum*: A comparative study with commercial drugs.

Anazodo, C. A., Adepeju, D. M., Okoli, F. A., Obasi, C. J., Abana, C. C., Agu, K. C., Ezenwelu, C. O., Awari, V. G., &Umeoduagu, N. D. (2024). Investigating the susceptibility of otomycosis-causing microorganisms to different ear drops. *International Research Journal of*

Modernization in Engineering Technology and Science, 6(6), 1958–1965.

Archer, G. L. (2018). *Staphylococcus aureus*: A well-armed pathogen. *Clinical Infectious Diseases*.

Ashishie, P. B., Anyama, C. A., Ayi, A. A., Oseghale, C. O., Adesuji, E. T., &Labulo, A. H. (2017). Green synthesis of silver monometallic and copper–silver bimetallic nanoparticles using *Kigeliaafricana* fruit extract and evaluation of their antimicrobial activities. *International Journal of Physical Sciences*, 13(3), 24–32.

Awah, N. S., Agu, K. C., Ikedinma, J. C., Uzoechi, A. N., Eneite, H. C., Victor-Aduloju, A. T., Umeoduagu, N. D., Onwuatuegwu, J. T. C., &Ilikannu, S. O. (2017). Antibacterial activities of aqueous and ethanolic extracts of male and female *Carica papaya* leaves. *Bioengineering and Bioscience*, 5(2), 25–29. https://doi.org/10.13189/bb.2017.050201

Awah, N. S., Agu, K. C., Okorie, C. C., Okeke, C. B., Iloanusi, C. A., Irondi, C. R., Udemezue, O. I., Kyrian-Ogbonna, A. E., Anaukwu, C. G., Eneite, H. C., Ifediegwu, M. C., Umeoduagu, N. D., Abah, N. H., &Ekong, U. S. (2016). *In vitro* assessment of the antibacterial quality of herbal and non-herbal toothpastes on *Streptococcus mutans*. *Open Journal of Dentistry and Oral Medicine*, 4(2), 21–25. https://doi.org/10.13189/ojdom.2016.040201

Awari, V. G., Umeoduagu, N. D., Agu, K. C., Okonkwo, N. N., &Chidozie, C. P. (2024). Antibiogram of pathogenic *Pseudomonas aeruginosa* isolated from hospital environment. *International Refereed Journal of Engineering and Science*, 13(2), 1–10.

Awari, V. G., Umeoduagu, N. D., Agu, K. C., Okonkwo, N. N., Ozuah, C. L., & Victor-Aduloju, A. T. (2023). The ubiquity, importance and harmful effects of microorganisms: An environmental and public health perspective. *International Journal of Progressive Research in Engineering Management and Science*, 3(12), 1–10.

Banin, E., Brady, K. M., & Greenberg, E. P. (2006). Chelator-induced dispersal and killing of *Pseudomonas aeruginosa* cells in a biofilm. *Applied and Environmental Microbiology*, 72(3), 2064–2069.

Buzea, C., Blandino, P. I. I., & Robbie, K. (2007). Nanomaterials and nanoparticles: Sources and toxicity. *Biointerphases*, 4(2), 17–172.

Das, J., &Velusamy, P. (2013). Biogenic synthesis of antifungal silver nanoparticles using aqueous stem extract of banana. *Nano Biomedicine and Engineering*, 5(1), 34–38.

Desmard, M., Davidge, K. S., Bouvet, O., Morin, D., Roux, D., Foresti, R., Ricard, J. D., Denamur, E., Poole, R. K., Montravers, P., Motterlini, R., &Boczkowski, J. (2009). A carbon monoxide-releasing molecule exerts bactericidal activity against *Pseudomonas aeruginosa*. *The FASEB Journal*, 23, 1023–1031.

Ekundayo, F. O., Oladipupo, O. A., &Ekundayo, E. A. (2013). Effects of microbial fermentation on bush mango (*Irvingiagabonensis*) seed cotyledons. *African Journal of Microbiology Research*, 7(34), 4363–4367.

Etta, H. E., Olisaeke, C. C., &Iboh, C. I. (2014). Effects of *Irvingiagabonensis* seeds on liver and gonads of male albino rats. *Journal of Biology, Agriculture and Healthcare*, 4(1), 10–16.

Ewere, E. G., Uka, E., &Usunobun, U. (2016). Phytochemical composition, antioxidant activity and acute toxicity of *Irvingiagabonensis*ethanolic leaf extract. *International Journal of Biological Research*, 4(1), 36–41.

Gellatly, S. E. W., & Hancock, R. (2013). *Pseudomonas aeruginosa*: New insights into pathogenesis and host defenses. *Pathogens and Disease*, 67, 159–173.

Gurunathan, S., Han, J. W., Dayem, A. A., Eppakayala, V., & Kim, J. (2012). Oxidative stress-mediated antibacterial activity of graphene oxide against

Pseudomonas aeruginosa. *International Journal of Nanomedicine*, 7, 5901–5914.

Hauser, A. R. (2009). The type III secretion system of *Pseudomonas aeruginosa*. *Nature Reviews Microbiology*, 7, 654–665.

Ingale, A. G., &Chaudhari, A. N. (2013). Biogenic synthesis of nanoparticles and potential applications. *Journal of Nanomedicine and Nanotechnology*, 4(2), 1–7.

Jena, J., Pradhan, N., Dash, B. P., Panda, P. K., & Mishra, B. K. (2015). Pigment-mediated biogenic synthesis of silver nanoparticles and antimicrobial activity. *Journal of Saudi Chemical Society*, 19, 661–666.

Kalaiyarasu, T., Karthi, N., Sharmila, G. V., & Manju, V. (2016). Antioxidant and antibacterial activity of green synthesized silver nanoparticles. *Asian Journal of Pharmaceutical and Clinical Research*, 9(1), 297–302.

Kim, S., Lee, H., Ryu, D., Choi, S., & Lee, D. (2011). Antibacterial activity of silver nanoparticles against *Staphylococcus aureus* and *Escherichia coli*. *Korean Journal of Microbiology and Biotechnology*, 39(1), 77–85.

Lateef, A., Azeez, M. A., Asafa, T. B., Yekeen, T. A., Akinboro, A., Oladipo, I. C., Azeez, L., Ajibade, S. E., Ojo, S. A., Gueguim-Kana, E. B., &Beukes, L. S. (2016). Biogenic synthesis of silver nanoparticles using *Cola nitida*. *Journal of Taibah University for Science*, 10, 551–562.

Mittal, A. K., Chisti, Y., & Banerjee, U. C. (2013). Synthesis of metallic nanoparticles using plant extracts. *Biotechnology Advances*, 31, 346–356.

Morones, J. R., Elechiguerra, J. L., Camacho, A., Holt, K., Kouri, J. B., Ramírez, J. T., &Yacaman, M. J. (2005). The bactericidal effect of silver nanoparticles. *Nanotechnology*, 16, 2346–2353.

Siddiqi, S. S., Husen, A., & Rao, R. A. K. (2018). Biosynthesis of silver nanoparticles and their biocidal properties. *Journal of Nanobiotechnology*, 16, 1–8.

Zolfaghari, P. S., Packer, S., Singer, M., Nair, S. P., Bennett, J., Street, C., & Wilson, M. (2009). *In vivo* killing of *Staphylococcus aureus* using a light-activated antimicrobial agent. *BMC Microbiology*, 9, 1–9.

Access this Article in Online	
Quick Response Code	Website: www.ijarbs.com
	Subject: Nanobiotechnology
DOI:10.22192/ijarbs.2026.13.01.001	

How to cite this article:
Anene I.C., Emejulu A.A., Anene C.C. , Oghonim P.AN, Ovowa O.F., Victor-Aduloju A.T., Abana, C.C., Egwuatu C.I. , Umeoduagu N.D., Okonkwo N.N., Ebo P.U. Igwilo C.Q. and Agu, K.C. (2026). Antimicrobial effects of *Irvingia gabonensis* peel extract-synthesized silver nanoparticles. Int. J. Adv. Res. Biol. Sci. 13(1): 1-15.
DOI: http://dx.doi.org/10.22192/ijarbs.2026.13.01.001